

Journal of Mechanics of Materials and Structures

**EFFECT OF SURFACE ELASTICITY
ON STRESS INTENSITY FACTORS
NEAR MODE-III CRACK TIPS**

Xian-Fang Li

Volume 14, No. 1

January 2019



EFFECT OF SURFACE ELASTICITY ON STRESS INTENSITY FACTORS NEAR MODE-III CRACK TIPS

XIAN-FANG LI

This paper studies a nanoscale mode-III crack in a homogeneous isotropic material. Classical elasticity, incorporating surface elasticity, is applied to solve a mixed boundary value problem. An emphasis is placed on the influence of surface elasticity on the stress intensity factors. Using the Fourier transform, the problem is reduced to a hypersingular integro-differential equation, then to a singular integro-differential equation with Cauchy kernel or a weakly singular integral equation with logarithmic kernel of the second kind. Using the Galerkin method, a solution of the resulting singular integro-differential equation is determined through expanding the out-of-plane displacement jump across crack faces as a series of Chebyshev polynomials. The influences of surface material properties on the stress intensity factor are examined and displayed graphically. For most materials, the surface effect decreases the stress intensity factors and enhances the effective fracture toughness of most nanoscale materials with a crack.

1. Introduction

With the development of nano/micro-techniques in recent years, the mechanical behavior of small scale materials and structures is quite significant for better understanding structural integrity, reliability, and stability. In particular, some defects such as dislocations, grain boundaries, cracks, holes, etc., inevitably appear in these structures because of fabrication techniques. It is well recognized that for nano/micro-scale materials and structures, in addition to macro bulk materials, small scale parameters play a crucial role in affecting mechanical properties. For example, as a key elastic property, Young's modulus of carbon nanotubes and graphene are measured to reach 1 TPa or more [Wong et al. 1997; Lee et al. 2008], much larger than that for conventional materials. Fracture of graphene has been analyzed and commented [Zhang et al. 2014; 2015]. A prevailing point of view is that taking into account large specific surface area for a nano/micro-material, surface effects including surface elasticity and surface residual tension should be included in assessing the overall material properties [Sharma and Ganti 2004; Duan et al. 2005], although they are negligible as compared to those for macro bulk materials. In this field, Gurtin and Murdoch (GM) [Gurtin and Murdoch 1975; Gurtin et al. 1998] first introduced surface/interface elasticity along with surface residual stress to extend the classical theory of elasticity. Based on surface elasticity theory, Ru [2010] put forward a simple geometrical explanation of the GM surface elasticity theory and gave several simplified surface constitutive relations. Consideration of surface properties strongly affects static and dynamic response of nanoscale materials and structures [Wu et al. 2017; Chen et al. 2017; Xiao and Li 2018].

Keywords: nanoscale crack, surface elasticity, stress intensity factor, hypersingular integro-differential equation.

Based on the GM model, Dingreville et al. [2005] exploited the surface free energy to describe its effect on the elastic behavior of nanomaterials and derived an overall prediction of the material properties for an elastic bulk material with nanosized particles, wires, and films. By means of the complex potential method, based on the GM model, Mogilevskaya et al. [2008] studied the interaction of elastic fields of multiple circular nanoinhomogeneities or/and nanopores in a two-dimensional elastic medium. Wu [1999] solved the effect of surface stresses on deformation of an elliptical hole and found the surface stress to change stress intensity factors. Wang et al. [2008] examined the surface effects on the crack-tip stresses for both mode-I and mode-III cracks and found that when the curvature radius of a blunt crack front decreases to nanometers, surface energy strongly affects the stress intensities near the crack tip. For a mode-II nanoscale crack, Fu et al. [2008] gave a similar analysis. Using a double cantilever beam model, Wang et al. [2013] addressed the influence of surface residual tension on stress intensity factors at the crack tips. Nan and Wang [2012] analyzed that effect of crack face residual stress on the fracture of nanoscale materials. Yang et al. [2018] established a thin plate model with surface effect to simulate the growth of a nanoscale penny-shaped crack and derived an accurate expression for calculating size-dependent energy release rates. In a review paper, Duan et al. [2009] commented some progress of the classical theory of elasticity incorporating the GM model of surface elasticity. On the other hand, the fundamental solution of a concentrated force at the surface of a half-plane or half-space with consideration of surface stresses as well as surface elasticity has been obtained [Wang and Feng 2007; Gao et al. 2013; 2014], and this solution can be used to treat a class of contact problems related to surface elasticity. Hu et al. [Hu et al. 2018; Hu and Li 2018] solved mode-I and II crack and rigid inclusion problems for a thin-film with surface effect and derived a closed-form solution of surface properties-dependent stress intensity factors or stress singularity coefficients. Utilizing the complex potential method, Kim et al. [2009; 2011a; 2011b; 2011c] investigated the effects of surface elasticity for a classical mode-III crack embedded in a linearly elastic material or bimaterial and further extended their results to mode-I and mode-II (interface) cracks for plane deformation. They found that surface elasticity leads to the disappearance of singular stresses near the crack tip. On the contrary, Walton [Walton 2012; Kim et al. 2013] also examined the tip-field singularity of a crack and found a logarithmic singularity of stresses near the crack tip when surface elasticity of the crack faces is considered. The influence of the surface effect on the stress intensity factors for a nanoscale crack has been analyzed for a bridged crack and an arc-shaped crack by Wang and Schiavone [2016] and Wang [2015], who found a weak logarithmic singularity outside the crack and a strong square root singularity on the crack faces.

In this paper, we analyze the stress field near the crack tip for a nanoscale crack embedded in an elastic medium with surface elasticity. First, a routine approach via the Fourier integral transform technique is employed to reduce the problem to a singular integro-differential equation. By use of the Galerkin method, we construct an approximate solution. Obtained results show that surface properties affect the stress intensity factors. Numerical results illustrate the strong influence of surface material parameters on stress intensity factors for nano/microscale cracks. Finally, some conclusions are drawn.

2. Statement of the problem

For a homogeneous isotropic linear bulk material, the stress-strain relations are governed by [Lurie and Belyaev 2005]

$$\sigma_{ij} = \lambda \varepsilon_{ll} \delta_{ij} + 2\mu \varepsilon_{ij}, \quad (1)$$

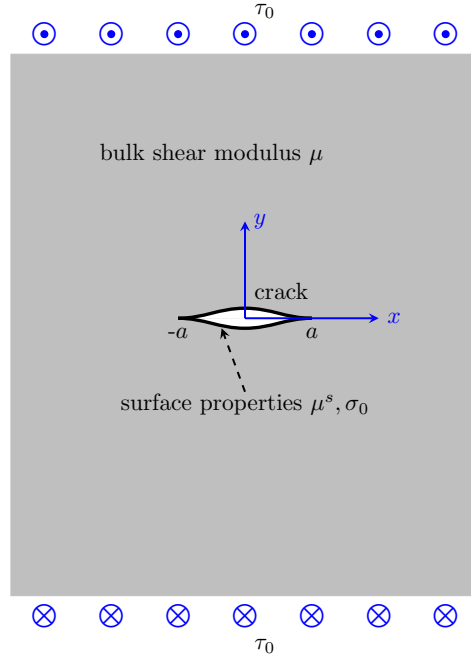


Figure 1. Schematic of a cracked medium with surface effect under remote antiplane shear loading.

where λ and μ are the Lamé constants, σ_{ij} is the Cauchy stress tensor, and ε_{ij} is the strain tensor. For a homogeneous isotropic surface material, the surface stress-strain relations read as follows [Gurtin and Murdoch 1975]:

$$\sigma_{\alpha\beta}^s = \sigma_0 \delta_{\alpha\beta} + (\lambda^s + \sigma_0) \varepsilon_{\gamma\gamma}^s \delta_{\alpha\beta} + 2(\mu^s - \sigma_0) \varepsilon_{\alpha\beta}^s + \sigma_0 u_{\alpha,\beta}^s, \quad (2)$$

$$\sigma_{\alpha 3}^s = \sigma_0 u_{3,\alpha}^s, \quad (3)$$

where λ^s and μ^s are the surface Lamé constants independent of the surface residual stress, σ_0 is the surface residual stress under unconstrained conditions, $\sigma_{\alpha j}^s$ are the Piola–Kirchhoff surface stresses, $\varepsilon_{\alpha\beta}^s$ are the surface strains, and u_α are the elastic displacement components. In the above, δ_{ij} or $\delta_{\alpha\beta}$ is the Kronecker delta, Latin subscripts i, j, l take values from 1 to 3, and Greek subscripts α, β, γ range from 1 to 2, a comma in the subscript denotes differentiation with respect to the spatial variable following the comma, and the Einstein convention of summation over repeated lower-case indices has been used.

In this paper a cracked material subjected to antiplane shear loading is studied, as shown in Figure 1. For convenience, a tunnel crack of length $2a$ is assumed to be located at the x -axis, i.e., $|x| < a$. In other words, in the present study we consider a nanoscale mode-III crack in plane strain state. Since antiplane shear loading is applied, there is only a unique out-of-plane displacement component, denoted as w and other displacement components along the x - and y -axes vanish. With w , the constitutive equation (1) for bulk material becomes

$$\sigma_{xz} = \mu \frac{\partial w}{\partial x}, \quad \sigma_{yz} = \mu \frac{\partial w}{\partial y}, \quad (4)$$

where μ denotes shear modulus of the material. Inserting the above constitutive equations for bulk material into the equilibrium equation

$$\frac{\partial \sigma_{xz}}{\partial x} + \frac{\partial \sigma_{yz}}{\partial y} = 0 \quad (5)$$

yields the following governing equation:

$$\frac{\partial^2 w}{\partial x^2} + \frac{\partial^2 w}{\partial y^2} = 0. \quad (6)$$

For a nanoscale mode-III crack embedded in a material, due to the presence of the crack, surface elasticity at the crack faces affects the mechanical behavior of a cracked material. To model a nanoscale crack, we adopt the surface elasticity formulated originally by Gurtin and Murdoch [1975]. Namely, the surface stresses of the crack faces satisfy the surface constitutive equations (2) and (3). They along with the bulk stresses satisfy the following equilibrium equations at the crack faces:

$$\llbracket \sigma_{ij} n_j e_i \rrbracket + \sigma_{\alpha\beta, \beta}^s e_\alpha = 0, \quad (7)$$

$$\llbracket \sigma_{ij} n_i n_j \rrbracket = \kappa_{\alpha\beta} \sigma_{\alpha\beta}^s, \quad (8)$$

where $\alpha, \beta = 1, 3$, $\kappa_{\alpha\beta}$ denotes the curvature tensor of surface, e_i is the unit vector component along the x_i direction, and $\llbracket * \rrbracket = (*)^+ - (*)^-$ stands for the jump of a quantity across the surface film. For the present problem under consideration, the above equilibrium equations (7) and (8) reduce to

$$\frac{\partial \sigma_{xx}^s}{\partial x} + \frac{\partial \sigma_{zx}^s}{\partial z} + \llbracket \sigma_{yx} \rrbracket = 0, \quad (9)$$

$$\frac{\partial \sigma_{xz}^s}{\partial x} + \frac{\partial \sigma_{zz}^s}{\partial z} + \llbracket \sigma_{yz} \rrbracket = 0, \quad (10)$$

$$\llbracket \sigma_{yy} \rrbracket = -\sigma_0 \left(\frac{\partial^2 v}{\partial x^2} + \frac{\partial^2 v}{\partial z^2} \right), \quad (11)$$

where v is the elastic displacement component along the y -axis. Only the out-of-plane displacement exists for an antiplane shear problem, and other displacement components are nil. Thus, using the surface stress-strain relation (2) with $\alpha = 1, \beta = 3$ or

$$\sigma_{xz}^s = (\mu^s - \sigma_0) \frac{\partial w}{\partial x}, \quad (12)$$

where μ^s is the surface shear modulus, σ_0 is the surface residual stress, and the surface displacement is assumed to be identical to that for the bulk displacement at a local position. From (9)–(11) we obtain

$$(\mu^s - \sigma_0) \frac{\partial^2 w}{\partial x^2} + \llbracket \sigma_{yz} \rrbracket = 0. \quad (13)$$

Finally, when applied loading at the crack faces is given, (13) can be rewritten as

$$\sigma_{yz}^\pm(x, 0) = q(x) \mp (\mu^s - \sigma_0) \frac{\partial^2 w(x, 0)}{\partial x^2}, \quad |x| < a, \quad (14)$$

where $q(x)$ is the prescribed loading at the crack faces. It represents the negative of applied antiplane shear loading without crack. Two typical cases are respectively analyzed in what follows. Case A

corresponds to an even loading $q_e(x)$ such as constant loading $-\tau_0$, which is equivalent to the application of a remote constant loading, and Case B corresponds to an odd loading $q_o(x)$ such as $-\tau_0 x/a$, which is equivalent to the application of a torque around the y -axis.

3. Derivation of singular integro-differential equation

This section is devoted to the derivation of singular integro-differential equation for the problem in question. To this end, we employ the Fourier transform technique to achieve our purpose. In addition to the boundary condition at the crack faces, we need to provide the boundary condition at the crack-free portion in the x -axis, i.e.,

$$w(x, 0) = 0, \quad |x| > a. \quad (15)$$

3.1. Case A. First the case of an even function loading $q_e(x)$ with respect to x is studied. Using the Fourier transform, we find that the out-of-plane displacement in the upper half-plane can be chosen as

$$w(x, y) = \frac{2}{\pi} \int_0^{\infty} A(\xi) \exp(-\xi y) \cos(\xi x) d\xi, \quad y \geq 0, \quad (16)$$

where $A(\xi)$ is an unknown function in ξ to be determined from the boundary conditions. Due to the symmetry of the problem, it is sufficient to determine the elastic field in the upper half-plane, and that in the lower half-plane can be directly written by symmetry. Plugging the expression (16) for the out-of-plane displacement into the constitutive relations (4) leads to an integral representation for the bulk stress components:

$$\sigma_{xz}(x, y) = -\frac{2\mu}{\pi} \int_0^{\infty} \xi A(\xi) \exp(-\xi y) \sin(\xi x) d\xi, \quad (17)$$

$$\sigma_{yz}(x, y) = -\frac{2\mu}{\pi} \int_0^{\infty} \xi A(\xi) \exp(-\xi y) \cos(\xi x) d\xi. \quad (18)$$

In order to derive a singular integro-differential equation, we define the so-called continuous screw dislocation pile-up or out-of-plane displacement jump across the crack faces as $2g(x)$, i.e.,

$$g(x) = w(x, 0). \quad (19)$$

Obviously, making use of the condition (15), one performs the Fourier cosine transform to (16) as $y = 0$. Thus we can express $A(\xi)$ in terms of $g(x)$ through the following integral:

$$A(\xi) = \int_0^a g(s) \cos(\xi s) ds. \quad (20)$$

Next, inserting (20) into (18) for $y = 0$ leads to

$$\sigma_{yz}(x, 0) = -\frac{2\mu}{\pi} \int_0^a g(s) ds \int_0^{\infty} \xi \cos(\xi s) \cos(\xi x) d\xi. \quad (21)$$

Recalling the well-known integral identity

$$\int_0^{\infty} \xi \cos(\xi x) \cos(\xi s) d\xi = -\frac{1}{2} \left[\frac{1}{(s+x)^2} + \frac{1}{(s-x)^2} \right], \quad (22)$$

we have

$$\sigma_{yz}(x, 0) = \frac{\mu}{\pi} \int_0^a g(s) \left[\frac{1}{(s+x)^2} + \frac{1}{(s-x)^2} \right] ds. \quad (23)$$

Considering that $g(x)$ is an even function, we immediately obtain

$$\int_0^a \frac{g(s)}{(s+x)^2} ds = \int_{-a}^0 \frac{g(s)}{(s-x)^2} ds, \quad (24)$$

and the stress (23) at the upper crack face is then rewritten as

$$\sigma_{yz}(x, 0) = \frac{\mu}{\pi} \int_{-a}^a \frac{g(s)}{(s-x)^2} ds. \quad (25)$$

Now we substitute (25) into the remaining boundary condition (14) at the upper crack face and get the following hypersingular integro-differential equation:

$$\frac{\mu}{\pi} \int_{-a}^a \frac{g(s)}{(s-x)^2} ds + (\mu^s - \sigma_0)g''(x) = q_e(x), \quad |x| < a, \quad (26)$$

where the double prime denotes second-order derivative with respect to x , and $q_e(x)$ is a prescribed even function. Due to the kernel $1/(s-x)^2$ having singularity of order 2, such a strongly singular integral equation with another differential term is called hypersingular integro-differential equation. Here, hypersingular integral is understood in the sense of Hadamard finite-part integral [Kaya and Erdogan 1987]. In fact, hypersingular integral equations have been widely used to tackle the classical crack problems [Ioakimidis 1982; Chan et al. 2003; Li 2003; Li et al. 2013]. In the above, besides the hypersingular integral term, the last term of the left-hand side of (26) is related to surface elasticity and it reflects the contribution of surface effect. Evidently, if neglecting the term related to $g''(x)$, the hypersingular integral equation for the classical mode-III crack is recovered. It is mentioned that if denoting $g'(x) = \eta(x)$, owing to $g(\pm a) = 0$ we perform integration by parts and get

$$\int_{-a}^a \frac{g(s)}{(s-x)^2} ds = \int_{-a}^a \frac{\eta(s)}{s-x} ds. \quad (27)$$

Thus the above equation (26) is equivalent to the following singular integro-differential equation:

$$(\mu^s - \sigma_0)\eta'(x) + \frac{\mu}{\pi} \int_{-a}^a \frac{\eta(s)}{s-x} ds = q_e(x), \quad (28)$$

identical to that obtained by Kim et al. [2009], who employed the complex variable method to derive the singular integro-differential equation (28) for a mode-III crack in an infinite elastic medium with surface elasticity. It is readily found that the unknown function $\eta(x)$ corresponds to the strain component physically. Strictly speaking, the behavior of $\eta(\pm a)$ is not obvious. In fact, it is the condition $\eta(\pm a) = 0$ that gives rise to no singularity occurring near the crack tips [Walton 2012; Kim et al. 2013]. Instead, for the unknown function $g(x)$ that stands for the displacement jump, the requirement of $g(\pm a) = 0$ is evident, which implies the single-value condition at the crack tips. As a consequence, although the singular integro-differential equation (28) is identical in form to that derived in [Kim et al. 2009], the

physical meaning of the unknown functions involved is completely different. A further simplification to (26) is achieved by integrating both sides of (26):

$$\frac{\mu}{\pi} \int_{-a}^a \frac{g(s)}{s-x} ds + (\mu^s - \sigma_0)g'(x) = \int_0^x q_e(s) ds, \quad |x| < a, \quad (29)$$

where a vanishing integration constant has been used since $g'(x)$ and $\int_{-a}^a g(s)/(s-x) ds$ are both odd functions with respect to x . Thus we have derived a singular integro-differential equation (29) for the out-of-plane displacement at the upper crack face $g(x)$, rather than its derivative $\eta(x)$.

3.2. Case B. In this subsection, we turn our attention to the case of antisymmetric odd loading $q_o(x)$. To treat this case, it is convenient to replace the out-of-plane displacement (16) by the following Fourier integral

$$w(x, y) = \frac{2}{\pi} \int_0^\infty B(\xi) \exp(-\xi y) \sin(\xi x) d\xi, \quad y \geq 0, \quad (30)$$

where $B(\xi)$ is an unknown function in ξ to be determined from the boundary conditions. In a similar manner, using the constitutive relations, we have the bulk stress components

$$\sigma_{xz}(x, y) = \frac{2\mu}{\pi} \int_0^\infty \xi B(\xi) \exp(-\xi y) \cos(\xi x) d\xi, \quad (31)$$

$$\sigma_{yz}(x, y) = -\frac{2\mu}{\pi} \int_0^\infty \xi B(\xi) \exp(-\xi y) \sin(\xi x) d\xi. \quad (32)$$

Under the same notation $g(x) = w(x, 0)$, $B(\xi)$ can be expressed in terms of $g(x)$ through the following integral:

$$B(\xi) = \int_0^a g(s) \sin(\xi s) ds, \quad (33)$$

which is inserted back into (32) for $y = 0$, giving

$$\sigma_{yz}(x, 0) = -\frac{2\mu}{\pi} \int_0^a g(s) ds \int_0^\infty \xi \sin(\xi s) \sin(\xi x) d\xi. \quad (34)$$

With the aid of the well-known integral identity

$$\int_0^\infty \xi \sin(\xi s) \sin(\xi x) d\xi = \frac{1}{2} \left[\frac{1}{(s+x)^2} - \frac{1}{(s-x)^2} \right], \quad (35)$$

we have

$$\sigma_{yz}(x, 0) = -\frac{\mu}{\pi} \int_0^a g(s) \left[\frac{1}{(s+x)^2} - \frac{1}{(s-x)^2} \right] ds. \quad (36)$$

Considering the fact that $g(x)$ is an odd function, we immediately obtain

$$\int_0^a \frac{g(s)}{(s+x)^2} ds = - \int_{-a}^0 \frac{g(s)}{(s-x)^2} ds, \quad (37)$$

and the stress (36) at the upper crack face is then rewritten as

$$\sigma_{yz}(x, 0) = \frac{\mu}{\pi} \int_{-a}^a \frac{g(s)}{(s-x)^2} ds. \quad (38)$$

Note that the above result is the same as (25). So applying the boundary condition at the upper crack face, the following hypersingular integro-differential equation can be derived:

$$\frac{\mu}{\pi} \int_{-a}^a \frac{g(s)}{(s-x)^2} ds + (\mu^s - \sigma_0)g''(x) = q_o(x), \quad |x| < a. \quad (39)$$

After integrating both sides of the above equation, one gets

$$\frac{\mu}{\pi} \int_{-a}^a \frac{g(s)}{s-x} ds + (\mu^s - \sigma_0)g'(x) = \int_0^x q_o(s) ds + C, \quad |x| < a, \quad (40)$$

where C denotes an integration constant. Differing from the previous result in the foregoing subsection, C does not vanish, but must be determined through the following supplementary condition, i.e.,

$$C = \frac{\mu}{\pi} \int_{-a}^a \frac{g(s)}{s} ds + (\mu^s - \sigma_0)g'(0). \quad (41)$$

As a result, we have also derived a singular integro-differential equation (40) but with an unknown constant C , which satisfies the condition (41).

4. Solution to the singular integro-differential equation

In order to derive the solution of the resulting integro-differential equation, we introduce the following dimensionless quantities:

$$\bar{g}(\bar{x}) = \frac{g(x)}{a}, \quad \theta = \frac{\mu^s - \sigma_0}{a\mu}, \quad (42)$$

$$q(x) = \tau_0 \bar{q}(\bar{x}), \quad \int_0^x q(s) ds = \tau_0 \zeta(\bar{x}) - C, \quad (43)$$

$$\bar{x} = \frac{x}{a}, \quad \bar{s} = \frac{s}{a}, \quad (44)$$

where $\zeta(\bar{x})$ is a prescribed function, which may contain an undetermined constant to ensure that the right-hand side vanishes as $\bar{x} = 0$. That is, we require $\zeta(0) \neq 0$ and it satisfies (41) for an even function $\zeta(\bar{x})$ corresponding to the case of an odd loading. The resulting equations for Cases A and B can be written as a unified form

$$\theta g''(\bar{x}) + \frac{1}{\pi} \int_{-1}^1 \frac{\bar{g}(\bar{s})}{(\bar{s} - \bar{x})^2} d\bar{s} = \frac{\tau_0}{\mu} \bar{q}(\bar{x}), \quad |\bar{x}| < 1, \quad (45)$$

or

$$\theta \bar{g}'(\bar{x}) + \frac{1}{\pi} \int_{-1}^1 \frac{\bar{g}(\bar{s})}{\bar{s} - \bar{x}} d\bar{s} = \frac{\tau_0}{\mu} \zeta(\bar{x}), \quad |\bar{x}| < 1. \quad (46)$$

The former is a hypersingular integro-differential equation, and the latter is a singular integro-differential equation.

Since the out-of-plane displacement at the upper crack face vanishes at both crack tips, i.e.,

$$\bar{g}(\pm 1) = 0, \quad (47)$$

we still give an alternative weakly singular integral equation with logarithmic kernel as follows:

$$\theta \bar{g}'(\bar{x}) - \frac{1}{\pi} \int_{-1}^1 \bar{g}'(\bar{s}) \ln|\bar{s} - \bar{x}| d\bar{s} = \frac{\tau_0}{\mu} \zeta(\bar{x}), \quad |\bar{x}| < 1. \quad (48)$$

The asymptotic behavior of the unknown function $\bar{g}(\bar{x})$ near the crack tips is, however, still unknown. As a consequence, a key task is to seek a solution to (46) subject to (47). Prior to the presentation of an appropriate solution, let us have a glance at the behavior of the solution to (46) subject to (47). If the parameter θ is sufficiently large, implying that the second term on the left-hand side of (46) is negligible as compared to the first term, after removing the second term one integrates both sides of (46) with respect to \bar{x} and finds that $\bar{g}(\bar{x})$ has a behavior like $(1 - \bar{x}^2)$ near $\bar{x} = \pm 1$ in view of $\zeta(0) \neq 0$. Conversely, if the parameter θ is sufficiently small, implying that the first term on the left-hand side of (46) is negligible as compared to the second term, after removing the first term (46) reduces to a standard singular integral equation with Cauchy kernel of the first kind, the solution of which under the condition (47) has a square-root behavior like $\sqrt{1 - \bar{x}^2}$ near $\bar{x} = \pm 1$ [Muskhelishvili 1977]. In fact, this conclusion may be seen from what follows. By rewriting (46) as

$$\frac{1}{\pi} \int_{-1}^1 \frac{\bar{g}(\bar{s})}{\bar{s} - \bar{x}} d\bar{s} = \frac{\tau_0}{\mu} \zeta(\bar{x}) - \theta \bar{g}'(\bar{x}), \quad (49)$$

with the well-known solution of a singular integral equation with the Cauchy kernel of the first kind [Muskhelishvili 1977, p. 155], by virtue of (47) we arrive at that the solution $\bar{g}(\bar{x})$ should satisfy the following relations:

$$\bar{g}(\bar{x}) = -\frac{\sqrt{1 - \bar{x}^2}}{\mu\pi} \int_{-1}^1 \frac{\tau_0 \zeta(\bar{s}) - \mu\theta \bar{g}'(\bar{s})}{(\bar{s} - \bar{x})\sqrt{1 - \bar{s}^2}} d\bar{s} \quad (50)$$

and

$$\int_{-1}^1 \frac{\tau_0 \zeta(\bar{s}) - \mu\theta \bar{g}'(\bar{s})}{\sqrt{1 - \bar{s}^2}} d\bar{s} = 0. \quad (51)$$

Based on the above analysis, we reasonably approximate the out-of-plane displacement $\bar{g}(\bar{x})$ by the following finite-term sum of the Chebyshev polynomials of the second kind [Frankel 1995; Bhattacharya and Mandal 2008]:

$$\bar{g}_N(\bar{x}) = \frac{\tau_0}{\mu} \sqrt{1 - \bar{x}^2} \sum_{n=0}^N b_n U_n(\bar{x}), \quad (52)$$

where the coefficients b_n are unknown coefficients, and N is a positive integer. Due to the completeness of $U_n(\bar{x})$, N is often chosen so large that the sum of the first finite terms converges the desired one, i.e., $\bar{g}_N(\bar{x}) \rightarrow \bar{g}(\bar{x})$ as $N \rightarrow \infty$. Hereafter we still denote $\bar{g}_N(\bar{x})$ as $\bar{g}(\bar{x})$, if no confusion is caused. Notice that if $\bar{g}_N(\bar{x})$ is even, only even terms $U_{2n}(\bar{x})$ are maintained in (52), whereas if $\bar{g}_N(\bar{x})$ is odd, only odd terms $U_{2n+1}(\bar{x})$ remain. In the above, the Chebyshev polynomial of the second kind $U_n(\bar{x})$ is defined as

$$U_n(\bar{x}) = \frac{\sin[(n+1)\cos^{-1}\bar{x}]}{\sin(\cos^{-1}\bar{x})}, \quad n \geq 0. \quad (53)$$

We stress that the assumption of the expression (52) is completely different from those used in [Kim et al. 2009; Wang 2015]. A solution in the form (52) is based on the out-of-plane displacement at the

upper crack face, not its derivative. Besides, different from most derivations, we use the Chebyshev polynomials of the second kind, not the first kind, and such a choice greatly simplifies the derivation. It is mentioned that an analogous expression of using the Chebyshev polynomial of the second kind has been applied in [Paulino et al. 2003]. Of course, it is also feasible to choose an expansion of the Chebyshev polynomials of the first kind such as $\bar{g}'_N(\bar{x}) = \mu^{-1}\tau_0 \sum_{n=0}^N b_n T_n(\bar{x})/\sqrt{1-\bar{x}^2}$ in place of (52), and we don't go on along this approach.

The remaining task is to determine the unknown coefficients b_n . We substitute the expansion (52) into (46), yielding

$$\sum_{n=0}^N b_n \left\{ \theta \frac{d}{d\bar{x}} [\sqrt{1-\bar{x}^2} U_n(\bar{x})] + \frac{1}{\pi} \int_{-1}^1 \frac{\sqrt{1-\bar{s}^2} U_n(\bar{s})}{\bar{s}-\bar{x}} d\bar{s} \right\} = \zeta(\bar{x}), \quad |\bar{x}| < 1. \quad (54)$$

Taking account of the following properties of derivatives and integrals involving the Chebyshev polynomials:

$$\frac{d}{d\bar{x}} [U_n(\bar{x})\sqrt{1-\bar{x}^2}] = -\frac{(n+1)T_{n+1}(\bar{x})}{\sqrt{1-\bar{x}^2}}, \quad |\bar{x}| < 1, \quad (55)$$

$$\frac{1}{\pi} \int_{-1}^1 \frac{U_n(\bar{s})\sqrt{1-\bar{s}^2}}{\bar{s}-\bar{x}} d\bar{s} = -T_{n+1}(\bar{x}), \quad |\bar{x}| < 1, \quad (56)$$

where $T_n(\bar{x})$ is the Chebyshev polynomial of the first kind, defined by

$$T_n(\bar{x}) = \cos(n \cos^{-1} \bar{x}), \quad n \geq 0, \quad (57)$$

one finds that (54) reduces to

$$\sum_{n=0}^N b_n \left[\frac{(n+1)\theta}{\sqrt{1-\bar{x}^2}} + 1 \right] T_{n+1}(\bar{x}) = -\zeta(\bar{x}), \quad |\bar{x}| < 1. \quad (58)$$

After multiplying both sides of (58) by $T_{m+1}(\bar{x})$, we then integrate both sides with respect to \bar{x} from -1 to 1 . Applying the orthogonality of the Chebyshev polynomials:

$$\int_{-1}^1 \frac{T_m(\bar{x})T_n(\bar{x})}{\sqrt{1-\bar{x}^2}} d\bar{x} = \begin{cases} 0, & m \neq n, \\ \pi, & m = n = 0, \\ \frac{1}{2}\pi, & m = n, m \neq 0, \end{cases} \quad (59)$$

and the closed-form integral formula

$$\int_{-1}^1 T_m(\bar{x})T_n(\bar{x}) d\bar{x} = \frac{1+(-1)^{m-n}}{2} \left[\frac{1}{1-(m-n)^2} + \frac{1}{1-(m+n)^2} \right], \quad (60)$$

we obtain linear algebraic equations for the unknown constants b_n ($n = 0, 1, \dots, N$):

$$\sum_{n=0}^N \left[\frac{(n+1)\theta\pi}{2} \delta_{mn} + a_{mn} \right] b_n = f_m, \quad m = 0, 1, 2, \dots, N, \quad (61)$$

where δ_{mn} denotes the Kronecker delta symbol, and

$$a_{mn} = \frac{1 + (-1)^{m-n}}{2} \left[\frac{1}{1 - (m-n)^2} + \frac{1}{1 - (m+n+2)^2} \right], \quad (62)$$

$$f_m = - \int_{-1}^1 \zeta(\bar{x}) T_{m+1}(\bar{x}) d\bar{x}. \quad (63)$$

For the case of an even loading, (61) forms a system of $(N+1)$ linear algebraic equations with $(N+1)$ unknowns. Solving the above system through a standard method, one gets the desired solution. For the case of an odd loading, an additional unknown constant C appears in (40), which can be determined by another supplementary condition (41). In other words, besides the above $N+1$ equations (61) we must add another equation, i.e.,

$$\sum_{n=0}^N b_n [(n+1)\theta + 1] \cos \frac{(1+n)\pi}{2} = -\zeta(0). \quad (64)$$

Therefore, (61) together with (64) form a system of $(N+2)$ linear algebraic equations with $(N+2)$ unknowns including $b_n(0, 1, 2, \dots, N)$ and $\zeta(0)$. Thus the resulting system is uniquely solvable.

Once the unknown coefficients b_n are determined, the stress singularity near the crack tips is readily derived. To this end, substituting (52) into (25) we get the stress along the crack line through the following integral:

$$\sigma_{yz}(x, 0) = \frac{\tau_0}{\pi} \sum_{n=0}^N b_n \int_{-1}^1 \frac{U_n(\bar{s}) \sqrt{1 - \bar{s}^2}}{(\bar{s} - \bar{x})^2} d\bar{s}. \quad (65)$$

Remembering the following properties of the Chebyshev polynomials [Paulino et al. 2003]:

$$\frac{1}{\pi} \int_{-1}^1 \frac{U_n(\bar{s}) \sqrt{1 - \bar{s}^2}}{(\bar{s} - \bar{x})^2} d\bar{s} = \begin{cases} -(n+1)U_n(\bar{x}), & |\bar{x}| < 1, \\ (n+1)(|\bar{x}|/\sqrt{\bar{x}^2 - 1} - 1)(\bar{x} - \bar{x}/|\bar{x}| \sqrt{\bar{x}^2 - 1})^n, & |\bar{x}| > 1, \end{cases} \quad (66)$$

for $n \geq 0$, we have

$$\sigma_{yz}(x, 0) = \tau_0 \sum_{n=0}^N b_n (n+1) \left(\frac{|\bar{x}|}{\sqrt{\bar{x}^2 - 1}} - 1 \right) \left(\bar{x} - \frac{\bar{x}}{|\bar{x}|} \sqrt{\bar{x}^2 - 1} \right)^n, \quad |\bar{x}| > 1. \quad (67)$$

From the above stress field, we find that the stress field exhibits the usual inverse square-root singularity near the crack tips. If defining the stress intensity factor by

$$K_{III}^+ = \lim_{x \rightarrow a^+} \sqrt{2\pi(x-a)} \sigma_{yz}(x, 0), \quad K_{III}^- = \lim_{x \rightarrow -a^-} \sqrt{-2\pi(a+x)} \sigma_{yz}(x, 0), \quad (68)$$

we can give the explicit expression for stress intensity factor as

$$K_{III}^+ = \tau_0 \sqrt{\pi a} \sum_{n=0}^N (n+1) b_n, \quad K_{III}^- = \tau_0 \sqrt{\pi a} \sum_{n=0}^N (-1)^n (n+1) b_n. \quad (69)$$

To get the stress distribution, from (25) and (46) one acquires the stress at the crack-free part:

$$\sigma_{yz}(x, 0) = \tau_0 \sum_{n=0}^N (n+1)b_n [x/a - x/|x|\sqrt{(x/a)^2 - 1}]^{n+1} [\sqrt{(x/a)^2 - 1}]^{-1}, \quad |x| > a. \quad (70)$$

It is obvious from the above result that bulk stress still exhibits an inverse square-root singularity unless $b_0 \neq 0$. This conclusion is different from the previous results. The reason is that Kim et al. [2009; 2011b] assumed a vanishing out-of-plane displacement gradient at the crack tips and found no singularity at the crack tips. Their treatment in fact corresponds to $b_0 = 0$. Finally, it is worth noting that on account of the influence of surface stress, the bulk stresses at the crack faces are not equal to applied loading at the crack faces. Or rather, using (38) and (39) one gets the bulk stress at the crack faces in the upper half-plane:

$$\sigma_{yz}(x, 0^+) = -\tau_0 \left\{ 1 - \theta \sum_{n=0}^N b_n (n+1) \left[\frac{(n+1)aU_n(x/a)}{\sqrt{a^2 - x^2}} + \frac{a^2 x T_{n+1}(x/a)}{(a^2 - x^2)^{3/2}} \right] \right\}, \quad |x| < a, \quad (71)$$

where in deriving the above result, (55) and

$$\frac{dT_{n+1}(x)}{dx} = (n+1)U_n(x) \quad (72)$$

have been used. It is readily found that because of consideration of surface effect, the bulk stress at the crack face exhibits a singular behavior near the crack tips, rather than a constant, although applied antiplane shear loading is uniform. When the surface effect is neglected, i.e., $\theta = 0$, applied constant loading is recovered, as expected.

5. Numerical results and discussion

In this section, numerical examples are presented to examine the influence of surface effect on stress intensity factors, crack face displacement, and stress distribution. In addition to bulk shear modulus μ , only the parameter θ enters the final equation (46). It indicates that all surface parameters including surface elasticity and surface residual stress in connection with crack length are combined into a dimensionless parameter θ .

We first examine the influence of the parameter θ on the stress intensity factors. As such, the following numerical results are only presented for uniform loading, i.e., $q(x) = -\tau_0$. Under such circumstances, we have $\zeta(\bar{x}) = -\bar{x}$ and (61) becomes

$$\sum_{n=0}^N \left[\frac{(2n+1)\pi}{2} \theta \delta_{mn} + \frac{1}{1-4(m-n)^2} + \frac{1}{1-4(m+n+1)^2} \right] b_n = \frac{2}{3-4m(1+m)}, \quad m=0, 1, \dots, N. \quad (73)$$

It is clear that the coefficients b_n are dependent on the parameter θ alone. By solving the above linear equations, the b_n are determined and the stress intensity factors are evaluated by (69). According to the estimate of Kim et al. [2009], the range of θ is not in excess of 0.1. Considering the occurrence of a negative parameter θ [Hu et al. 2018], Table 1 examines the convergence of the numerical results of the normalized stress intensity factor $K_{III}/\tau_0\sqrt{\pi a}$ for various values of θ . From Table 1, one finds that if taking $\theta = 10^{-8}$, meaning that surface effect is nearly negligible, the normalized stress intensity factors

$\theta \downarrow$	$N \rightarrow 20$	40	60	80	100
-10^{-4}	1.06148	1.28376	1.9920	9.87854	-
-10^{-6}	1.00058	1.00217	1.0048	1.00848	1.01324
-10^{-8}	1.00001	1.00002	1.00005	1.00008	1.00013
0	1	1	1	1	1
10^{-8}	0.999994	0.999978	0.999952	0.999916	0.999869
10^{-6}	0.999424	0.997837	0.995247	0.991669	0.987129
10^{-4}	0.945787	0.824715	0.686202	0.562309	0.462943
10^{-3}	0.646534	0.357601	0.230787	0.168227	0.132117
10^{-2}	0.206562	0.0998366	0.0659344	0.0492867	0.039375
10^{-1}	0.0561862	0.0284717	0.0190879	0.0143603	0.0115109

Table 1. The normalized stress intensity factor $K_{III}^+/\tau_0\sqrt{\pi a}$.

are almost equal to unity. Since θ is inversely proportional to the crack length, as shown in (42), that is to say that when the crack length arrives at a macroscale such as centimeter or larger, the value of θ is close to 10^{-8} , and the classical stress intensity factor is then recovered. Moreover, for such θ values, the convergence of the numerical results is very satisfactory. However, with the crack length decreasing, or θ rising, we find that the influence of surface effect is enhanced, and the normalized stress intensity factors obviously decline if the same term number N is chosen. It implies that when the crack length drops, the surface effect gives rise to a reduction of the stress intensity factor. That is, consideration of the surface effect enhances apparent fracture toughness of the material. This conclusion agrees well with theoretical prediction [Wang et al. 2013; Yang et al. 2018] and some experimental observation [Gojny et al. 2004; Kim et al. 2008; Liu et al. 2011]. Additionally, for a given θ value, $\theta = 0.001$, say, one views that the evaluated normalized stress intensity factors take 0.65 for $N = 20$ and 0.13 for $N = 100$, respectively. That implies that the convergence rate becomes quite slow, particularly for larger values of θ . This conclusion is attributed to the contribution of the first term of the left-hand side of (46) containing an unbounded derivative operator, which plays an amplification role for small values, particularly when the term number is large enough. This characteristic belongs to the nature of the derivative operator. For most cases, θ is positive. However, for a few cases with a negative θ value, the stress intensity factors increase with θ being larger in magnitude, which is capable of promoting crack growth or decreasing apparent fracture toughness. In the following, $N = 100$ is chosen unless otherwise stated.

If the coefficients b_n are determined by solving the resulting algebraic equations, the dimensionless out-of-plane displacement $\mu\bar{g}(\bar{x})/\tau_0$ is numerically calculated through the expansion (52), and the corresponding profiles at the upper crack-face are plotted in Figure 2 for several different θ values. From Figure 2, one finds that when θ is less than 10^{-3} , the profile curve of the dimensionless out-of-plane displacement $\mu\bar{g}(\bar{x})/\tau_0$ almost does not vary. For larger values such as $\theta = 0.05, 0.1$, the profile curve has a relatively large deviation.

Figure 3 shows the variation of bulk stress $\sigma_{zy}(x, 0)/\tau_0$ as a function of x for various values of θ . From Figure 3, it is seen that the bulk stress nearly takes a constant at the crack face ($|x| < a$) and the influence of surface effect is undetectable since the dimensionless parameter $\theta = 10^{-8}$ is sufficiently small. If setting $\theta = 0$, the bulk stress at the crack face identically takes a constant -1 , which reduces

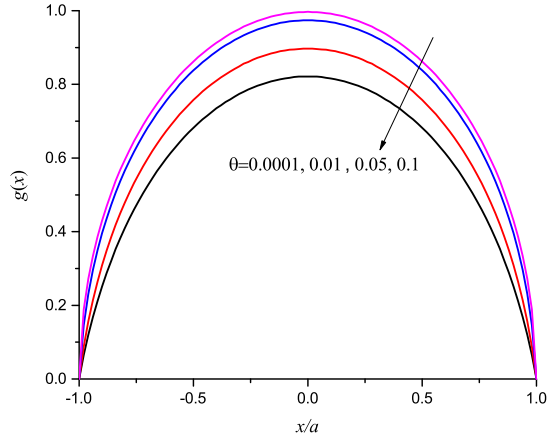


Figure 2. Profile of the dimensionless out-of-plane displacement $\mu\bar{g}(\bar{x})/\tau_0$ at the upper crack-face.

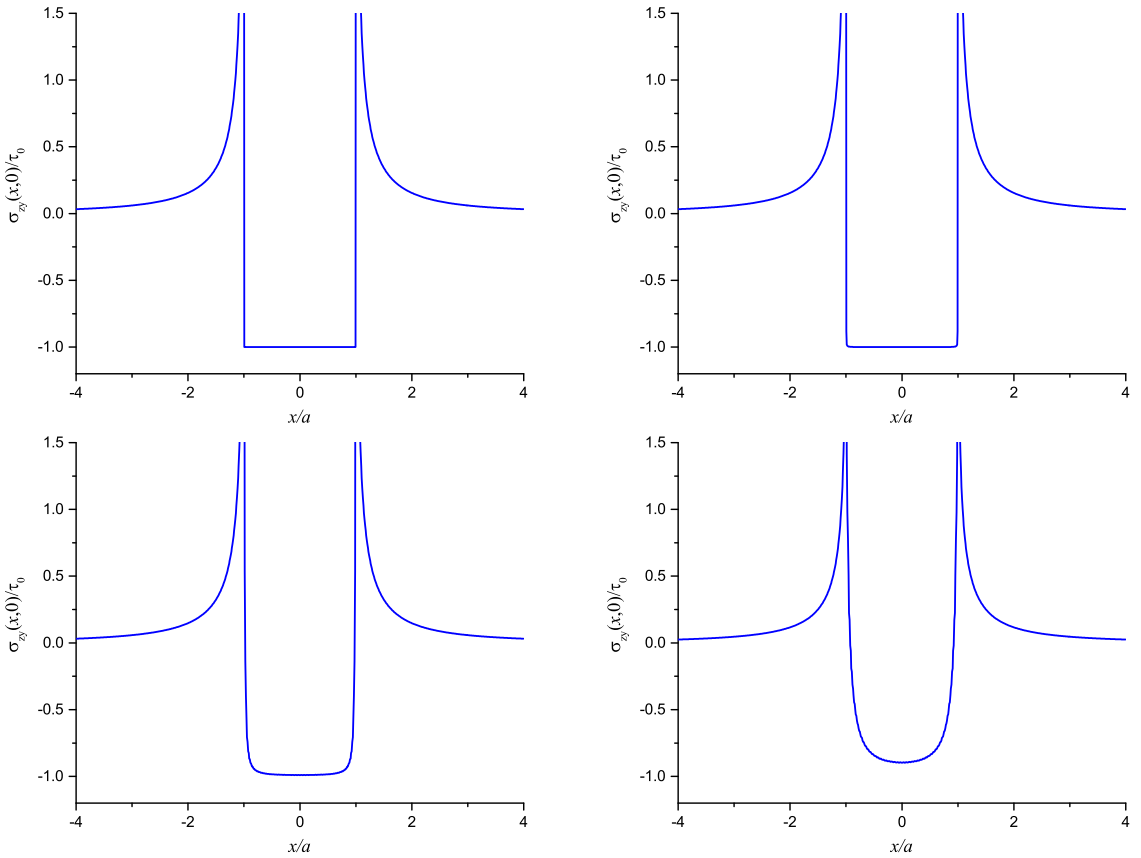


Figure 3. The variation of bulk stress $\sigma_{zy}(x, 0)/\tau_0$ as a function of x for various values of θ . Top left: $\theta = 10^{-8}$. Top right: $\theta = 10^{-4}$. Bottom left: $\theta = 10^{-2}$. Bottom right: $\theta = 10^{-1}$.

to the classical result. With θ rising, the surface effect alters the stress distribution. For example, for $\theta = 10^{-2}, 10^{-1}$, it is seen in Figure 3, bottom, that the bulk stress at the crack face varies. At the crack-free part, the bulk stress always exhibits inverse square-root singularity, as shown in Figure 3.

For practical situations, the θ values need to be given beforehand. Usually, bulk and surface material properties cover a large range. For example, the material properties of GaN, composed of a mixture of nitrified aluminum (Al), gallium (Ga) and indium (In) take the following values: $1.7 \text{ GPa} \leq \mu \leq 168 \text{ GPa}$, $0.7 \text{ N/m} < \sigma_0 < 2 \text{ N/m}$, $\mu^s = 161.73 \text{ J/m}^2$ [Sharma and Ganti 2004]. A copper single crystal with $E = 123.5 \text{ GPa}$, 11.6 N/m , $\sigma_0 = 1.5 \text{ N/m}$ [Choi et al. 2010], and an anodic alumina with $E = 70 \text{ GPa}$, $E^s = 5.19 \text{ N/m}$, $\sigma_0 = 0.91 \text{ N/m}$ [Shenoy 2005]. Therefore, in what follows we consider several typical values of $(\mu^s - \sigma_0)/\mu$, reflecting the surface characteristic length, and plot the variation of the stress intensity factors against the crack half-length a in Figure 4. From Figure 4, left, we see that for those materials with $(\mu^s - \sigma_0)/\mu = 10^{-10} \text{ m}$, when the crack half-length is lower than $10 \mu\text{m}$, the surface effect comes into play and rapidly decreases the stress intensity factor, and when the crack half-length arrives at nanometer order, the stress intensity factor nearly equals zero, implying very weak singularity near the crack tips. In other words, the load-carrying capacity is effectively enhanced. Furthermore, if the surface shear modulus μ^s is raised, which causes $(\mu^s - \sigma_0)/\mu$ to rise, $(\mu^s - \sigma_0)/\mu = 10^{-8} \text{ m}$, say, one finds that the influence of surface effect is apparently observed for those cracks with length of millimeter order. Moreover, when the crack length drops to micrometer, the stress singularity almost disappears. This also sheds light on a mechanism that it is more difficult for micro/nanometer cracks to grow since the surface effect decreases the stress singularity and impedes crack advance. Or rather, the effective fracture toughness of cracked materials is enhanced when the crack length is reduced. This conclusion is verified by some experimental evidence. For example, Zhang et al. [2014] demonstrated that fracture stress is raised when the crack length is lowered for a bilayer graphene with a precrack. Cohen-Tanugi and Grossman [2014] showed an increase in fracture stress with nanopore radius decreasing in nanoporous graphene. Since most materials give a positive value of the parameter θ , it is worth noting that a negative value of θ for a few materials increases the stress intensity factors, as seen in Figure 4, right, which speeds crack advance. This trend is opposite to that for the case of $\theta > 0$.

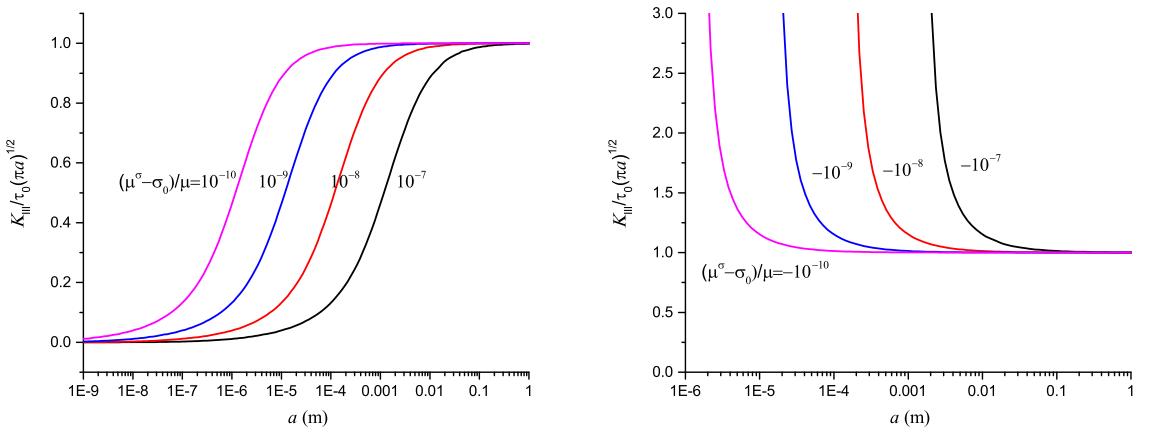


Figure 4. Dimensionless stress intensity factor $K_{III}/\tau_0\sqrt{\pi a}$ against the crack half-length a (m) for typical values of (left) positive and (right) negative $(\mu^s - \sigma_0)/\mu$ (m).

6. Conclusions

In this paper, we analyzed a mode-III crack embedded in an isotropic homogeneous medium with surface effect and examined the influence of surface material properties on a stress singularity near the crack tips. Using the Fourier transform, we first derived a hypersingular integro-differential equation. The Galerkin method was adopted to solve the resulting equation. Based on the expansion of the out-of-plane displacement jump across crack faces in terms of Chebyshev polynomials, the unknown coefficients were determined. The stress intensity factors were obtained and displayed for different surface properties. Obtained results show that for most materials with positive values of the parameter θ , consideration of surface effect decreases the stress intensity factors, or the effective fracture toughness is enhanced for materials with nano/microscale crack. Conversely, negative θ values increase the stress intensity factors or reduce the effective fracture toughness.

Acknowledgments

This work was supported by the National Natural Science Foundation of China (Grant No. 11672336). The author thanks the anonymous reviewers for their helpful suggestions for improving this paper.

References

- [Bhattacharya and Mandal 2008] S. Bhattacharya and B. N. Mandal, “Numerical solution of a singular integro-differential equation”, *Appl. Math. Comput.* **195**:1 (2008), 346–350.
- [Chan et al. 2003] Y.-S. Chan, A. C. Fannjiang, and G. H. Paulino, “Integral equations with hypersingular kernels: theory and applications to fracture mechanics”, *Int. J. Eng. Sci.* **41**:7 (2003), 683–720.
- [Chen et al. 2017] D. Q. Chen, D. L. Sun, and X.-F. Li, “Surface effects on resonance frequencies of axially functionally graded Timoshenko nanocantilevers with attached nanoparticle”, *Compos. Struct.* **173** (2017), 116–126.
- [Choi et al. 2010] J. Choi, M. Cho, and W. Kim, “Surface effects on the dynamic behavior of nanosized thin film resonator”, *Appl. Phys. Lett.* **97**:17 (2010), art. id. 171901.
- [Cohen-Tanugi and Grossman 2014] D. Cohen-Tanugi and J. C. Grossman, “Mechanical strength of a nanoporous graphene as a desalination membrane”, *Nano Lett.* **14**:11 (2014), 6171–6178.
- [Dingreville et al. 2005] R. Dingreville, J. Qu, and M. Cherkaoui, “Surface free energy and its effect on the elastic behavior of nano-sized particles, wires and films”, *J. Mech. Phys. Solids* **53**:8 (2005), 1827–1854.
- [Duan et al. 2005] H. L. Duan, J. Wang, Z. P. Huang, and B. L. Karihaloo, “Size-dependent effective elastic constants of solids containing nano-inhomogeneities with interface stress”, *J. Mech. Phys. Solids* **53**:7 (2005), 1574–1596.
- [Duan et al. 2009] H. L. Duan, J. Wang, and B. L. Karihaloo, “Theory of elasticity at the nanoscale”, *Adv. Appl. Mech.* **42** (2009), 1–68.
- [Frankel 1995] J. I. Frankel, “A Galerkin solution to a regularized Cauchy singular integro-differential equation”, *Quart. Appl. Math.* **53**:2 (1995), 245–258.
- [Fu et al. 2008] X. L. Fu, G.-F. Wang, and X. Q. Feng, “Surface effects on the near-tip stress fields of a mode-II crack”, *Int. J. Fract.* **151**:2 (2008), 95–106.
- [Gao et al. 2013] X. Gao, F. Hao, D. Fang, and Z. Huang, “Boussinesq problem with the surface effect and its application to contact mechanics at the nanoscale”, *Int. J. Solids Struct.* **50**:16-17 (2013), 2620–2630.
- [Gao et al. 2014] X. Gao, F. Hao, Z. Huang, and D. Fang, “Mechanics of adhesive contact at the nanoscale: the effect of surface stress”, *Int. J. Solids Struct.* **51**:3-4 (2014), 566–574.
- [Gojny et al. 2004] F. H. Gojny, M. H. G. Wichmann, U. Köpke, B. Fiedler, and K. Schulte, “Carbon nanotube-reinforced epoxy-composites: enhanced stiffness and fracture toughness at low nanotube content”, *Compos. Sci. Technol.* **64**:15 (2004), 2363–2371.

- [Gurtin and Murdoch 1975] M. E. Gurtin and A. I. Murdoch, “A continuum theory of elastic material surfaces”, *Arch. Ration. Mech. Anal.* **57** (1975), 291–323. Addenda in **59:4** (1975), 389–390.
- [Gurtin et al. 1998] M. E. Gurtin, J. Weismüller, and F. Larché, “A general theory of curved deformable interfaces in solids at equilibrium”, *Philos. Mag. A* **78:5** (1998), 1093–1109.
- [Hu and Li 2018] Z.-L. Hu and X.-F. Li, “A rigid line inclusion in an elastic film with surface elasticity”, *Z. Angew. Math. Phys.* **69:4** (2018), art. id. 92.
- [Hu et al. 2018] Z.-L. Hu, K. Y. Lee, and X.-F. Li, “Crack in an elastic thin-film with surface effect”, *Int. J. Eng. Sci.* **123** (2018), 158–173.
- [Ioakimidis 1982] N. I. Ioakimidis, “Application of finite-part integrals to the singular integral equations of crack problems in plane and three-dimensional elasticity”, *Acta Mech.* **45:1-2** (1982), 31–47.
- [Kaya and Erdogan 1987] A. C. Kaya and F. Erdogan, “On the solution of integral equations with strongly singular kernels”, *Quart. Appl. Math.* **45:1** (1987), 105–122.
- [Kim et al. 2008] B. C. Kim, S. W. Park, and D. G. Lee, “Fracture toughness of the nano-particle reinforced epoxy composite”, *Compos. Struct.* **86:1-3** (2008), 69–77.
- [Kim et al. 2009] C. I. Kim, P. Schiavone, and C.-Q. Ru, “The effects of surface elasticity on an elastic solid with mode-III crack: complete solution”, *J. Appl. Mech. (ASME)* **77:2** (2009), art. id. 021011.
- [Kim et al. 2011a] C. I. Kim, P. Schiavone, and C.-Q. Ru, “Analysis of plane-strain crack problems (mode-I and mode-II) in the presence of surface elasticity”, *J. Elasticity* **104:1-2** (2011), 397–420.
- [Kim et al. 2011b] C. I. Kim, P. Schiavone, and C.-Q. Ru, “The effect of surface elasticity on a mode-III interface crack”, *Arch. Mech. Stos.* **63:3** (2011), 267–286.
- [Kim et al. 2011c] C. I. Kim, P. Schiavone, and C.-Q. Ru, “Effect of surface elasticity on an interface crack in plane deformations”, *Proc. R. Soc. Lond. A* **467:2136** (2011), 3530–3549.
- [Kim et al. 2013] C. I. Kim, C.-Q. Ru, and P. Schiavone, “A clarification of the role of crack-tip conditions in linear elasticity with surface effects”, *Math. Mech. Solids* **18:1** (2013), 59–66.
- [Lee et al. 2008] C. Lee, X. Wei, J. W. Kysar, and J. Hone, “Measurement of the elastic properties and intrinsic strength of monolayer graphene”, *Science* **321:5887** (2008), 385–388.
- [Li 2003] X.-F. Li, “Electroelastic analysis of an internal interface crack in a half-plane consisting of two bonded dissimilar piezoelectric quarter-planes”, *Meccanica (Milano)* **38:3** (2003), 309–323.
- [Li et al. 2013] X.-F. Li, G.-J. Tang, and B.-Q. Tang, “Stress field around a strike-slip fault in orthotropic elastic layers via a hypersingular integral equation”, *Comput. Math. Appl.* **66:11** (2013), 2317–2326.
- [Liu et al. 2011] H.-Y. Liu, G.-T. Wang, Y.-W. Mai, and Y. Zeng, “On fracture toughness of nano-particle modified epoxy”, *Compos. B Eng.* **42:8** (2011), 2170–2175.
- [Lurie and Belyaev 2005] A. I. Lurie and A. Belyaev, *Theory of elasticity*, Springer, 2005.
- [Mogilevskaya et al. 2008] S. G. Mogilevskaya, S. L. Crouch, and H. K. Stolarski, “Multiple interacting circular nano-inhomogeneities with surface/interface effects”, *J. Mech. Phys. Solids* **56:6** (2008), 2298–2327.
- [Muskhelishvili 1977] N. I. Muskhelishvili, *Some basic problems of the mathematical theory of elasticity*, Springer, 1977.
- [Nan and Wang 2012] H. Nan and B. Wang, “Effect of residual surface stress on the fracture of nanoscale materials”, *Mech. Res. Commun.* **44** (2012), 30–34.
- [Paulino et al. 2003] G. H. Paulino, A. C. Fannjiang, and Y.-S. Chan, “Gradient elasticity theory for mode III fracture in functionally graded materials, I: Crack perpendicular to the material gradation”, *J. Appl. Mech. (ASME)* **70:4** (2003), 531–542.
- [Ru 2010] C.-Q. Ru, “Simple geometrical explanation of Gurtin–Murdoch model of surface elasticity with clarification of its related versions”, *Sci. China G Phys. Mech. Astronom.* **53:3** (2010), 536–544.
- [Sharma and Ganti 2004] P. Sharma and S. Ganti, “Size-dependent Eshelby’s tensor for embedded nano-inclusions incorporating surface/interface energies”, *J. Appl. Mech. (ASME)* **71:5** (2004), 663–671.
- [Shenoy 2005] V. B. Shenoy, “Atomistic calculations of elastic properties of metallic fcc crystal surfaces”, *Phys. Rev. B* **71:9** (2005), art. id. 094104. Correction in **74:14** (2006), art. id. 149901.

- [Walton 2012] J. R. Walton, “A note on fracture models incorporating surface elasticity”, *J. Elasticity* **109**:1 (2012), 95–102.
- [Wang 2015] X. Wang, “A mode III arc-shaped crack with surface elasticity”, *Z. Angew. Math. Phys.* **66**:4 (2015), 1987–2000.
- [Wang and Feng 2007] G.-F. Wang and X. Q. Feng, “Effects of surface stresses on contact problems at nanoscale”, *J. Appl. Phys.* **101**:1 (2007), art. id. 013510.
- [Wang and Schiavone 2016] X. Wang and P. Schiavone, “Bridged cracks of mode III with surface elasticity”, *Mech. Mater.* **95** (2016), 125–135.
- [Wang et al. 2008] G.-F. Wang, X.-Q. Feng, T.-J. Wang, and W. Gao, “Surface effects on the near-tip stresses for mode-I and mode-III cracks”, *J. Appl. Mech. (ASME)* **75**:1 (2008), art. id. 011001.
- [Wang et al. 2013] H. Wang, X. Li, G. Tang, and Z. Shen, “Effect of surface stress on stress intensity factors of a nanoscale crack via double cantilever beam model”, *J. Nanosci. Nanotechnol.* **13**:1 (2013), 477–482.
- [Wong et al. 1997] E. W. Wong, P. E. Sheehan, and C. M. Lieber, “Nanobeam mechanics: elasticity, strength, and toughness of nanorods and nanotubes”, *Science* **277**:5334 (1997), 1971–1975.
- [Wu 1999] C. H. Wu, “The effect of surface stress on the configurational equilibrium of voids and cracks”, *J. Mech. Phys. Solids* **47**:12 (1999), 2469–2492.
- [Wu et al. 2017] J.-X. Wu, X.-F. Li, A.-Y. Tang, and K. Y. Lee, “Free and forced transverse vibration of nanowires with surface effects”, *J. Vib. Control* **23**:13 (2017), 2064–2077.
- [Xiao and Li 2018] Q.-X. Xiao and X.-F. Li, “Flutter and divergence instability of rectangular plates under nonconservative forces considering surface elasticity”, *Int. J. Mech. Sci.* **149** (2018), 254–261.
- [Yang et al. 2018] Y. Yang, K. Y. Lee, and X.-F. Li, “Surface effects on delamination of a thin film bonded to an elastic substrate”, *Int. J. Fract.* **210**:1-2 (2018), 81–94.
- [Zhang et al. 2014] P. Zhang, L. Ma, F. Fan, Z. Zeng, C. Peng, P. E. Loya, Z. Liu, Y. Gong, J. Zhang, X. Zhang, P. M. Ajayan, T. Zhu, and J. Lou, “Fracture toughness of graphene”, *Nat. Commun.* **5** (2014), art. id. 3782.
- [Zhang et al. 2015] T. Zhang, X. Li, and H. Gao, “Fracture of graphene: a review”, *Int. J. Fract.* **196**:1-2 (2015), 1–31.

Received 18 Jul 2018. Revised 29 Nov 2018. Accepted 4 Dec 2018.

XIAN-FANG LI: xfli@csu.edu.cn

School of Civil Engineering, Central South University, Changsha, 410075, China

JOURNAL OF MECHANICS OF MATERIALS AND STRUCTURES

msp.org/jomms

Founded by Charles R. Steele and Marie-Louise Steele

EDITORIAL BOARD

ADAIR R. AGUIAR	University of São Paulo at São Carlos, Brazil
KATIA BERTOLDI	Harvard University, USA
DAVIDE BIGONI	University of Trento, Italy
MAENGHYO CHO	Seoul National University, Korea
HUILING DUAN	Beijing University
YIBIN FU	Keele University, UK
IWONA JASIUKEWICZ	University of Illinois at Urbana-Champaign, USA
DENNIS KOCHMANN	ETH Zurich
MITSUTOSHI KURODA	Yamagata University, Japan
CHEE W. LIM	City University of Hong Kong
ZISHUN LIU	Xi'an Jiaotong University, China
THOMAS J. PENCE	Michigan State University, USA
GIANNI ROYER-CARFAGNI	Università degli studi di Parma, Italy
DAVID STEIGMANN	University of California at Berkeley, USA
PAUL STEINMANN	Friedrich-Alexander-Universität Erlangen-Nürnberg, Germany
KENJIRO TERADA	Tohoku University, Japan

ADVISORY BOARD

J. P. CARTER	University of Sydney, Australia
D. H. HODGES	Georgia Institute of Technology, USA
J. HUTCHINSON	Harvard University, USA
D. PAMPLONA	Universidade Católica do Rio de Janeiro, Brazil
M. B. RUBIN	Technion, Haifa, Israel

PRODUCTION production@msp.org

SILVIO LEVY Scientific Editor


Cover photo: Ev Shafir

See msp.org/jomms for submission guidelines.

JoMMS (ISSN 1559-3959) at Mathematical Sciences Publishers, 798 Evans Hall #6840, c/o University of California, Berkeley, CA 94720-3840, is published in 10 issues a year. The subscription price for 2019 is US \$635/year for the electronic version, and \$795/year (+\$60, if shipping outside the US) for print and electronic. Subscriptions, requests for back issues, and changes of address should be sent to MSP.

JoMMS peer-review and production is managed by EditFLOW[®] from Mathematical Sciences Publishers.

PUBLISHED BY

 **mathematical sciences publishers**
nonprofit scientific publishing

<http://msp.org/>

© 2019 Mathematical Sciences Publishers

The role of rheology in modelling elastic waves with gas bubbles in granular fluid-saturated media	ADHAM A. ALI and DMITRY V. STRUNIN	1
Some general theorems for local gradient theory of electrothermoelastic dielectrics	OLHA HRYTSYNA and HALYNA MOROZ	25
Effect of surface elasticity on stress intensity factors near mode-III crack tips	XIAN-FANG LI	43
Analytical investigation of free vibrations of a bounded nonlinear bulk-elastic medium in a field of mass forces	EUGENE I. RYZHAK and SVETLANA V. SINYUKHINA	61
A modified shear-lag model for prediction of stress distribution in unidirectional fibrous composites considering interphase	MOHAMMAD HASSAN ZARE and MEHDI MONDALI	97
Nonlinear free vibration of nanobeams based on nonlocal strain gradient theory with the consideration of thickness-dependent size effect	WEI CHEN, LIN WANG and HU-LIANG DAI	119
Energy-maximizing holes in an elastic plate under remote loading	SHMUEL VIGDERGAUZ and ISAAC ELISHAKOFF	139
Anisotropic multimaterial lattices as thermal adapters	MARINA M. TOROPOVA	155
Thermal stress around an elliptic hole weakened by electric current in an infinite thermoelectric plate	KUN SONG, HAO-PENG SONG, PETER SCHIAVONE and CUN-FA GAO	179